Aromaticity and Conjugation in Sapphyrin and Orangarin

Jun-ichi Aihara[*1,2] **and Masakazu Makino**[2]

[1]Department of Chemistry, Faculty of Science, Shizuoka University, Oya, Shizuoka 422-8529

[2]Institute for Environmental Sciences, Shizuoka University, Yada, Shizuoka 422-8526

Received June 26, 2008; E-mail: scjaiha@yahoo.co.jp

We analyzed aromatic and magnetic properties of two typical expanded porphyrins, sapphyrin and orangarin, using our theory of aromaticity and ring-current diamagnetism and confirmed that, as in the case of free-base porphine, global aromaticity and macrocyclic circulation are associated primarily with five pyrrolic rings and the macrocyclic annulenoid pathway, respectively. For orangarin, the main pathway of macrocyclic circulation is different from the [20]annulene pathway so far proposed as a main macrocyclic conjugation pathway. A new method was proposed for associating the main macrocyclic conjugation pathway with the π-current density pattern.

Porphyrin chemistry is now in full bloom.[1–3] Many expanded, contracted, and confused porphyrins have so far been synthesized. Among the expanded porphyrins are sapphyrin (**1**) and orangarin (**2**) in Figure 1. The former is the first recorded expanded porphyrin,[4–6] whereas the latter, with two methine bridges in **1** replaced by direct links, is the smallest expanded porphyrin so far prepared.[7] Structural and magnetic characteristics of porphyrins have usually been accounted for by a formal analogy between main conjugation pathways in porphyrin macrocycles and simple annulenes.[8–10] For example, natural porphyrins are described as bridged diaza[18]annulenes. The same convention has been applied to many expanded porphyrins. Thus, **1** and **2** are regarded as aromatic [22]annulene[4,5,11] and antiaromatic [20]annulene derivatives,[7,11] respectively. Such an annulenoid picture of porphyrins is formally consistent with the observed chemical shifts of the methine and amine protons.[8–11]

In 1998–2002, three research groups re-investigated possible aromatic pathways in free-base porphine and metalloporphine.[12–14] They noted that not only conjugation along the porphine macrocycle but also local aromaticity of pyrrolic rings is important in determining the degree of global aromaticity. We then analyzed aromatic character of these porphines using our theory of aromaticity[15–21] and ring-current diamagnetism[22–29] and pointed out that four separate pyrrolic rings dominate global aromaticity.[30] However, this aspect of global aromaticity never depreciates the concept of macrocyclic aromaticity for porphyrins, which are closely related to the proton chemical shifts.[8–11] In this paper, we explore aromaticity and magnetotropicity of expanded porphyrins **1** and **2** in some detail. Here, diatropicity and paratropicity are referred to collectively as magnetotropicity. A new method is proposed for predicting the main macrocyclic conjugation pathway from the π-current density pattern.

Theoretical Background for the Present Study

The term "aromatic" describes molecules that benefit energetically from the delocalization of π-electrons in closed circuits.[31]

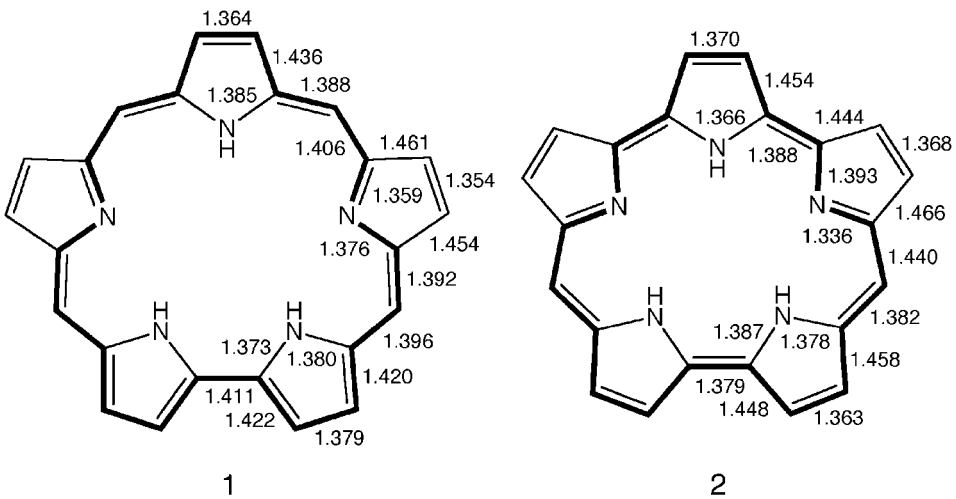

Figure 1. Sapphyrin (**1**) and orangarin (**2**) with B3LYP/6-31G**-optimized bond lengths in Å. Annulene pathways are shown in bold.

Published on the web June 12, 2009; doi:10.1246/bcsj.82.675

Topological resonance energy (TRE) is a kind of aromatic stabilization energy (ASE) and is used as a primary criterion of aromaticity.[15,16] Bond resonance energy (BRE) for a given π-bond represents the contribution of all circuits that share the bond to TRE.[19–21] Superaromatic stabilization energy (SSE) represents an extra ASE due to macrocyclic conjugation.[17,18,21] The term "superaromaticity" is used as a synonym of "macrocyclic aromaticity."

We below summarize our theory used to calculate ring-current diamagnetic susceptibilities and related quantities. It is an analytical variant[22–29] of Hückel–London theory.[32,33] Van-Catledge's set of Hückel parameters for heteroatoms[34] is employed. Bond-length alternation was not taken into consideration in our Hückel–London calculations. Molecular geometries employed are those optimized at the B3LYP/6-31G** level of theory using the Gaussian 03 suite of programs.[35]

Ring-Current Magnetic Susceptibility. Our theory allows a partitioning of the ring-current magnetic susceptibility for a polycyclic π-system exactly into separate circuit contributions. Here, circuits stand for all possible cyclic or closed paths that can be chosen from a cyclic π-system.[36]

We first calculate the value of A_i defined for each circuit in a polycyclic π-system:[22–25]

$$A_i = 4\prod_{m>n}^{r_i} k_{mn} \sum_{j}^{occ} \frac{P_{G-r_i}(X_j)}{P'_G(X_j)} \tag{1}$$

where r_i is a set of conjugated atoms and π-bonds that constitute the i-th circuit c_i; k_{mn} is the Hückel parameter for the resonance integral between atoms m and n; m and n run over all π-bonds that belong to c_i; $G - r_i$ is the subsystem of G obtained by deleting r_i from G; $P_G(X)$ and $P_{G-r_i}(X)$ are the characteristic polynomials for G and $G - r_i$, respectively; X_j is the j-th largest zero of $P_G(X)$; a prime added to $P_G(X)$ indicates the first derivative with respect to X; and j runs over all occupied π-molecular orbitals. If there are degenerate π-orbitals, eq 1 must be replaced by others.[22,24]

When an external magnetic field, H, is oriented perpendicular to the plane of G, the ring-current magnetic susceptibility is expressed in the form:[22–25]

$$\chi_G = 4.5\chi_0 \sum_{i}^{G} A_i \left(\frac{S_i}{S_0}\right)^2 \tag{2}$$

where χ_0 is the ring-current susceptibility of benzene; S_i and S_0 are the areas of r_i and the benzene ring, respectively; and i runs over all circuits in G. Positive and negative A_i values represent diamagnetic and paramagnetic contributions, respectively. The contribution of the i-th circuit to χ_G i.e., the circuit-current susceptibility, is then given as[22–25]

$$\chi_i = 4.5\chi_0 A_i \left(\frac{S_i}{S_0}\right)^2 \tag{3}$$

Circuit Current. A current induced in each circuit may be termed a circuit current. The i-th circuit-current susceptibility, χ_i, corresponds to the induction of a circuit current in the i-th circuit the intensity of which is given by:[25–27,37]

$$I_i = 4.5 I_0 A_i \frac{S_i}{S_0} \tag{4}$$

where I_0 is the intensity of a π-electron current induced in the benzene ring. Positive and negative A_i values now represent diatropic and paratropic currents, respectively. A current density map for an entire π-system is obtained by superposing all circuit currents. It is exactly the same as that obtained by the original Hückel–London procedure.[38,39]

Magnetic Resonance Energy. We have interpreted the A_i value successfully as a circuit contribution to ASE and termed it the i-th circuit resonance energy (CRE_i).[26–29] As can be seen from eq 3, circuit-current susceptibility, i.e., the tendency of a given circuit to escape from the magnetic field, is proportional to the CRE multiplied by the circuit area squared. As the A_i value can be interpreted as CRE_i, the sum of A_i values over all circuits can be interpreted as an ASE for an entire π-system. This quantity was termed magnetic resonance energy (MRE), which means a TRE-like resonance energy derived from the magnetic response of the π-system:[26–28]

$$\begin{aligned} MRE/|\beta| &= \sum_{i}^{G} A_i \\ &= \sum_{i}^{G} CRE_i/|\beta| \end{aligned} \tag{5}$$

For a variety of polycyclic aromatic hydrocarbons and heterocycles, MRE highly correlates with TRE.[26–28]

Results and Discussion

Sapphyrin (**1**) and orangarin (**2**) are pentaphyrins with 32π- and 30π-electrons, respectively. TREs and SSEs for **1** and **2** are listed in Table 1. For reference, TRE and SSE for free-base porphine are 0.4322 and 0.0843, respectively, both in units of $|\beta|$.[30] All these species are aromatic with positive TREs. For porphyrins, SSE is equal to the BRE for a CC bond that links any pair of adjacent pyrrolic rings.[21,30] SSE defined in this manner will be referred to as t-SSE, because it is a topologically defined quantity.[29] Another definition of SSE will be introduced later. Macrocyclic conjugation never gives a major contribution to the global aromaticity of a porphyrin π-system. Like free-base porphine,[30] **1** is slightly superaromatic with a small positive t-SSE, whereas **2** is slightly antisuperaromatic with a small negative t-SSE. BREs for **1** and **2** are graphically summarized in Figure 2. CC bonds in the five-membered rings exhibit larger positive BREs, which indicate again that the five-membered rings are the main source of aromaticity.

The BRE concept is also useful for identifying main macrocyclic conjugation pathways in porphyrins. We recently found that the main macrocyclic conjugation pathway in a porphyrin molecule can be traced by choosing a π-bond with a larger BRE at every bifurcation of the π-network.[21] Such a conjugation pathway is usually consistent with the observed proton chemical shifts.[21] All π-bonds located along such a macrocyclic conjugation pathway are intensified with larger positive BREs than those located along the bypasses. This never implies that macrocyclic conjugation dominates global aromaticity. For **1**, π-bonds with relatively large positive BREs are arranged along the [22]annulene or 22π-electron conjugation pathway, which can therefore be considered as a main macrocyclic conjugation pathway.

Table 1. TREs and t-SSEs for Sapphyrin and Orangarin

Species	TRE/$\lvert\beta\rvert$	t-SSE/$\lvert\beta\rvert$
Sapphyrin (**1**)	0.5904	0.0639
Orangarin (**2**)	0.5656	−0.0696

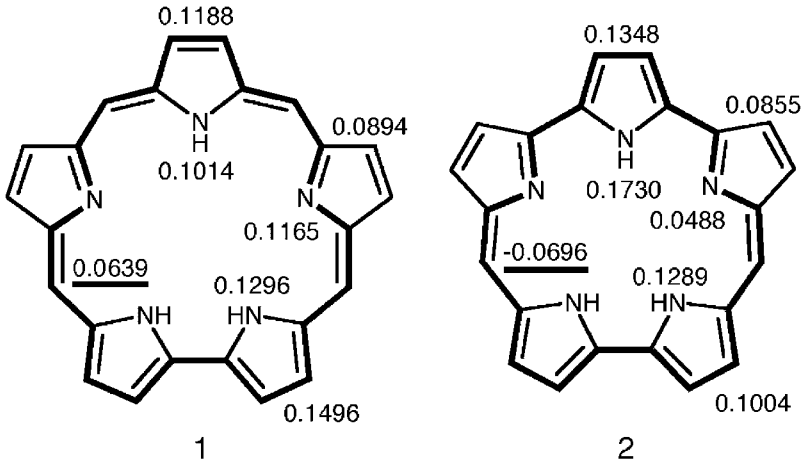

Figure 2. Bond resonance energies (BREs) in units of $|\beta|$ for **1** and **2**. The underlined BREs correspond to *t*-SSEs. Macrocyclic conjugation or destabilization pathways are shown in bold, which are identical with the annulene pathways in Figure 1.

However, such an aromatic annulene pathway does not exist in the macrocycle of **2**, because it is not a superaromatic species. Instead, an antiaromatic [20]annulene or 20π-electron pathway can be traced by choosing a π-bond with a smaller BRE at every bifurcation of the π-network. All π-bonds located along such an antiaromatic annulene pathway are weakened with smaller BREs than those located along the bypasses. A macrocyclic pathway thus determined is consistent with the paramagnetic ring-current. Note that not only the aromatic [22]annulene pathway in **1** but also the antiaromatic [20]annulene pathway in **2** is a conjugated circuit in Randić's terminology.[40] Therefore, the latter will also be referred to as a main macrocyclic conjugation pathway. Main macrocyclic conjugation pathways thus determined for **1** and **2** are exactly the same as the annulene pathways accepted by porphyrin chemists. These pathways are shown in bold in Figures 1 and 2. The signs of the SSEs for **1** and **2** are consistent with these annulene-like pictures.

We next examine aromaticity and ring-current diamagnetism of **1** and **2** in terms of π-electron circuits. As shown in Figure 3, **1** has 23 non-identical circuits and a total of 37 circuits. The first five are five-site ones located along the five pyrrolic rings. The rest of the circuits are located along the macrocycle that encloses the inner cavity. Except for the fact that **2** has two less methine carbon atoms, relative positions of five five-membered rings are the same in **1** and **2**. Therefore, the same lower-case letters **a**–**w** can be assigned to structurally analogous circuits in the two π-systems. For example, **a**, **b**, and **c** represent three types of five-site circuits in **1** and **2**, while **d** represents the circuits that can be chosen along the inner peripheries of these π-systems.

CREs calculated for all non-identical circuits in **1** and **2** are listed in Table 2. Here, the multiplicity stands for the number of identical circuits. All of the five-site circuits in **1** and **2** exhibit the largest positive CREs, supporting the view that the pyrrolic rings dominate the aromaticity of the entire π-system. In general, larger circuits have smaller positive or negative CREs.[22,27] As in the case of free-base porphine,[30] all local and macrocyclic circuits in **1** are aromatic with positive CREs. In contrast, all macrocyclic circuits in **2** are antiaromatic with negative CREs, although all local circuits are aromatic. It is these macrocyclic circuits that are responsible for the macrocyclic antiaromaticity in **2**. Circuit **q** in **1** represents the circuit that can be chosen along the main conjugation pathway and hence has the largest positive CRE among the macrocyclic circuits, whereas circuit **q** in **2** represents the circuit that can be chosen along the main conjugation pathway and has the largest negative CRE among the macrocyclic circuits.

MREs and magnetic SSEs (*m*-SSEs) for **1** and **2** are presented in Table 3. Here, *m*-SSE stands for an SSE derived from the magnetic response of the π-system, which is given as a sum of CREs for all macrocyclic circuits.[21] For reference, MRE and *m*-SSE for free-base porphine are 0.3390 and 0.0686, respectively, both in units of $|\beta|$. In general, MRE correlates in magnitude with TRE.[26–28] For the two porphyrins, *m*-SSE is close in value to *t*-SSE. Therefore, global and macrocyclic aromaticity can likewise be estimated from the MRE and *m*-SSE, respectively. It may be noteworthy that MRE for **2** is appreciably larger than that for **1**, although TRE for **2** is smaller than that for **1**. In fact, a correlation between TRE and MRE is deteriorated for antiaromatic species.[41] Even for polycyclic π-systems with antiaromatic substructures, calculated magnetic properties are very sensitive to the molecular geometry and the molecular orbital method employed.[42–44] Relatively large MRE for **2** may possibly reflect macrocyclic antiaromaticity.

Intensities of circuit currents for **1** and **2**, each expressed as a multiple of the benzene value, are added in Table 2. The plus and minus signs indicate diamagnetic and paramagnetic currents, respectively. According to eq 4, the intensity of each circuit current is proportional not only to the CRE but also to the area enclosed by the circuit. All five-site circuits sustain intense diamagnetic currents because the CREs are very large. All macrocyclic circuits have more than eight times as large areas as that of any pyrrolic ring, so must be responsible collectively for the strong π-currents induced along the macrocycle. However, these circuits are far from being a main source of global aromaticity, because their CREs are very small. A macrocyclic circuit that sustains the strongest current is circuit **q** both in **1** and **2**, which are consistent with the annulenoid pictures for these expanded porphyrins.

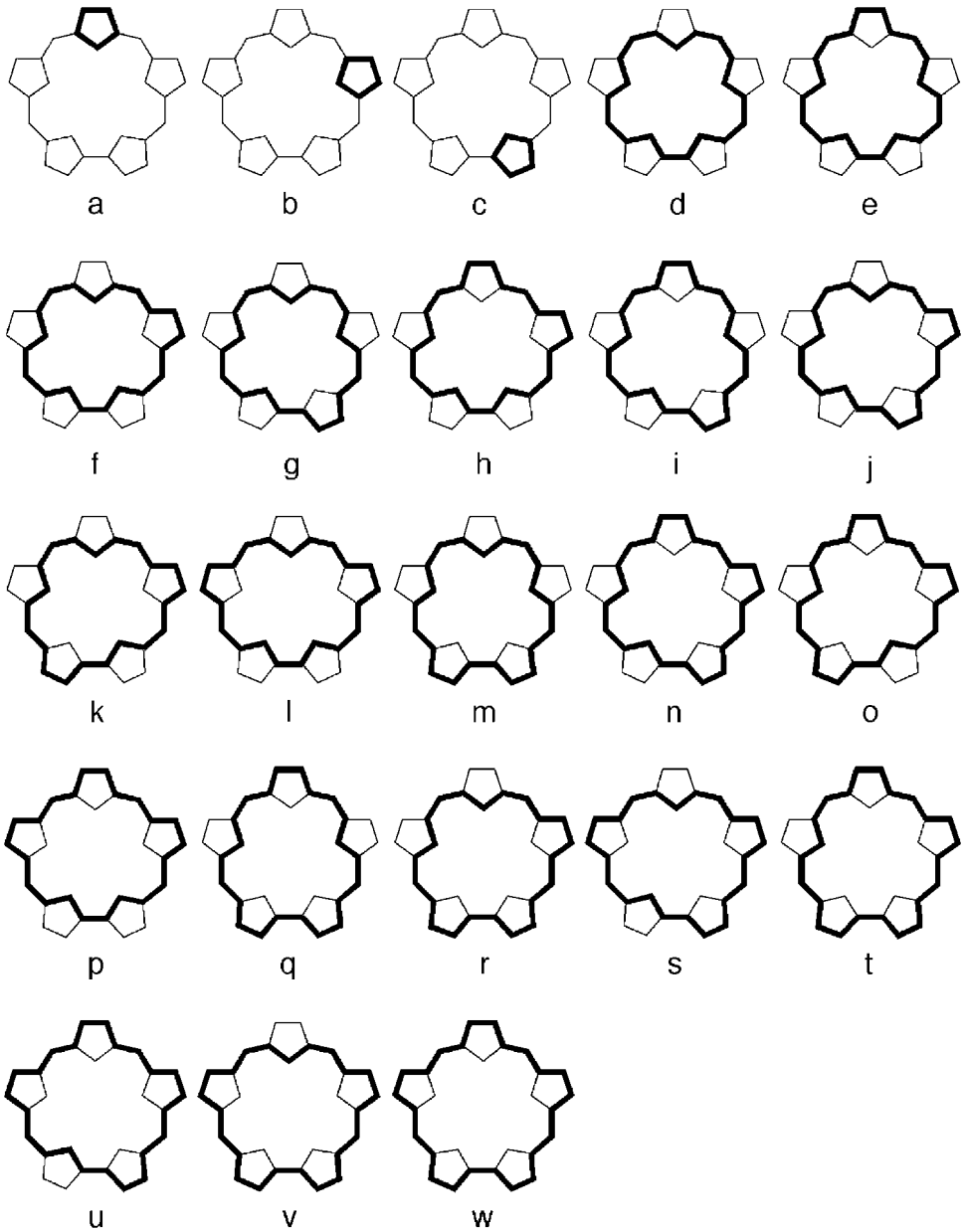

Figure 3. Non-identical circuits in **1**.

π-Current density maps for **1** and **2**, obtained by superposing all circuit currents concerned, are presented in Figure 4. Here, counterclockwise and clockwise circulations represent diatropic and paratropic ring currents, respectively. In harmony with the sign of the SSE, a diamagnetic current runs through the methine carbons in **1**, whereas a paramagnetic current runs through the methine carbons in **2**. The main stream of the ring-current in **1** runs along the [22]annulene pathway, which passes through two imine (=N–) nitrogens but avoids three amine (–NH–) nitrogens. However, the main stream of the ring-current in **2** runs along the inner periphery, passing through all nitrogen atoms. This aspect of macrocyclic circulation is not consistent with the [20]annulene conjugation pathway.

Steiner and Fowler[11] carried out practical ring-current calculations on **1** and **2** with the 6-31G** basis by means of coupled Hartree–Fock theory within the ipsocentric[45,46] CTOCD-DZ (continuous transformation of origin of current density-diamagnetic zero) formulation.[47,48] Both molecules give clearly dominant macrocyclic currents, but in opposite directions; intense diamagnetic and paramagnetic currents are induced along the macrocycles of **1** and **2**, respectively. Sapphyrin (**1**) was predicted to sustain a strong diamagnetic current along the [22]annulene pathway, whereas orangarin (**2**) was predicted to sustain a strong paramagnetic current along the inner periphery.[11] This paratropic circulation follows, not the conventional [20]annulene pathway, but the innermost shortest possible, 17-atom pathway around the macrocycle (i.e., the inner periphery), with only weak current density on peripheral CC bonds.

As seen from Figure 4, our ring-current calculation reproduces the main circulation pathways that Steiner and Fowler predicted for **1** and **2**.[11] In both ring-current calculations,

Table 2. Circuit Resonance Energies (CREs), Circuit Currents, and Circuit-Current Diamagnetic Susceptibilities for Sapphyrin and Orangarin

Circuit	Area $/S_0$	Multiplicity	CRE $/\|\beta\|$	Circuit current $/I_0$	Circuit-current diamagnetic susceptibility $/\chi_0$
A. Sapphyrin (**1**)					
a	0.6627	1	0.0759	0.2262	0.1499
b	0.6615	2	0.0773	0.2300	0.1522
c	0.6573	2	0.0992	0.2933	0.1928
d	7.3723	1	0.0013	0.0419	0.3090
e	8.0350	1	0.0022	0.0794	0.6384
f	8.0339	2	0.0006	0.0221	0.1774
g	8.0296	2	0.0022	0.0794	0.6375
h	8.6966	2	0.0011	0.0418	0.3635
i	8.6923	2	0.0037	0.1437	1.2487
j	8.6912	2	0.0011	0.0418	0.3630
k	8.6912	2	0.0011	0.0418	0.3630
l	8.6954	1	0.0002	0.0092	0.0804
m	8.6869	1	0.0037	0.1436	1.2472
n	9.3538	2	0.0017	0.0704	0.6587
o	9.3538	2	0.0017	0.0704	0.6587
p	9.3581	1	0.0005	0.0209	0.1953
q	9.3496	1	0.0061	0.2581	2.4127
r	9.3484	2	0.0017	0.0704	0.6579
s	9.3527	2	0.0005	0.0209	0.1950
t	10.0111	2	0.0027	0.1233	1.2347
u	10.0154	2	0.0007	0.0297	0.2976
v	10.0100	1	0.0007	0.0297	0.2973
w	10.6727	1	0.0011	0.0541	0.5774
B. Orangarin (**2**)					
a	0.6506	1	0.1884	0.5516	0.3589
b	0.6602	2	0.1344	0.3993	0.2636
c	0.6547	2	0.1516	0.4467	0.2924
d	5.6892	1	−0.0023	−0.0579	−0.3292
e	6.3398	1	−0.0038	−0.1079	−0.6841
f	6.3494	2	−0.0010	−0.0300	−0.1903
g	6.3438	2	−0.0038	−0.1080	−0.6850
h	7.0000	2	−0.0017	−0.0533	−0.3733
i	6.9944	2	−0.0063	−0.1969	−1.3772
j	7.0040	2	−0.0017	−0.0534	−0.3737
k	7.0040	2	−0.0017	−0.0534	−0.3737
l	7.0096	1	−0.0004	−0.0141	−0.0991
m	6.9985	1	−0.0063	−0.1970	−1.3788
n	7.6546	2	−0.0027	−0.0935	−0.7155
o	7.6546	2	−0.0027	−0.0935	−0.7155
p	7.6602	1	−0.0007	−0.0237	0.1818
q	7.6491	1	−0.0102	−0.3520	−2.6926
r	7.6587	2	−0.0027	−0.0935	−0.7162
s	7.6642	2	−0.0007	−0.0237	−0.1820
t	8.3093	2	−0.0043	−0.1608	−1.3358
u	8.3148	2	−0.0011	−0.0402	−0.3340
v	8.3189	1	−0.0011	−0.0402	−0.3344
w	8.9695	1	−0.0016	−0.0663	−0.5945

Table 3. MREs and *m*-SSEs for Sapphyrin and Orangarin

Species	MRE/$\|\beta\|$	*m*-SSE/$\|\beta\|$
Sapphyrin (**1**)	0.4817	0.0530
Orangarin (**2**)	0.6733	−0.0871

macrocyclic circulations in **1** and **2** are diamagnetic and paramagnetic, respectively. Our simple calculation somewhat overestimates the intensity of paramagnetic currents that flow on the CC bonds of the pyrrolic rings in **2**. This must possibly be due to the neglect of bond-length alternation that occurs along the [20]annulene pathway. As shown in Figure 1, the degree of bond-length alternation along the main macrocyclic conjugation pathway is a bit more pronounced in **2** than in **1**. Bond lengths given in this figure are those optimized at the B3LYP/6-31G** level of theory using the Gaussian 03 suite of programs.[35]

We found that a discrepancy found between the main macrocyclic conjugation and main circulation pathways in the orangarin macrocycle can be interpreted in terms of circuit currents. For porphyrins in general, a main macrocyclic π-circulation pathway and the conventional annulene pathway are two different manifestations of macrocyclic conjugation. In this context, one should note that local circulations in pyrrolic rings are superposed on macrocyclic circulation. In the case of sapphyrin (**1**), a diamagnetic current is induced along the macrocycle; it is bifurcated when it passes through every pyrrolic ring. A strong diamagnetic current is also induced in every five-site circuit. Both diamagnetic currents flow in the same direction on the outer CC bonds of the pyrrolic rings. However, both diamagnetic currents totally or partially cancel each other out on the inner CN bonds of the pyrrolic rings, because both currents flow in opposite directions. Thus, local circulations may obscure the main stream of macrocyclic circulation.

On the other hand, orangarin (**2**) sustains a paramagnetic current along the macrocycle. It is bifurcated when it passes through every pyrrolic ring. In addition, a strong diamagnetic current is induced in every five-site circuit. Both paramagnetic and diamagnetic currents flow in opposite directions on the outer CC bonds of the pyrrolic rings and so totally or partially cancel each other out there. However, both currents flow in the same direction on the inner CN bonds of the pyrrolic rings. As a result, the intensified clockwise current is observed on the inner CN bonds. This must be the main reason why apparently strong paramagnetic circulation in **2** follows the inner periphery. Presumably, such an effect of local circulations on the current density map is pronounced when the macrocycle sustains a paramagnetic current.

Therefore, if one wants to trace macrocyclic circulation alone, the circulation of π-electrons along the macrocycle only must be extracted from the global current density. Fortunately, π-current density is an additive function of all circuits. As shown in Figure 5, the entire ring current in **1** can be partitioned into the contribution of macrocyclic circuits (**1A**) and that of the five-site circuits (**1B**). Likewise, the entire ring-current in **2** can be partitioned into the contribution of macrocyclic circuits (**2A**) and that of the five-site circuits (**2B**). One now sees that the main macrocyclic circulation

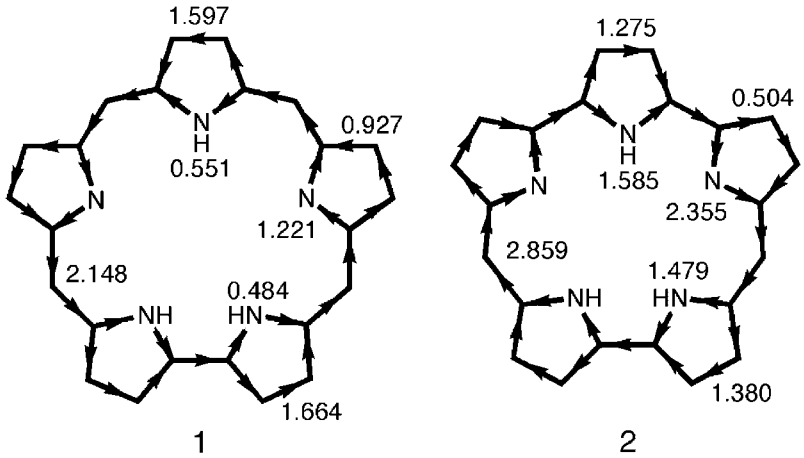

Figure 4. π-Current density maps for **1** and **2**. All current intensities are given in units of the benzene value.

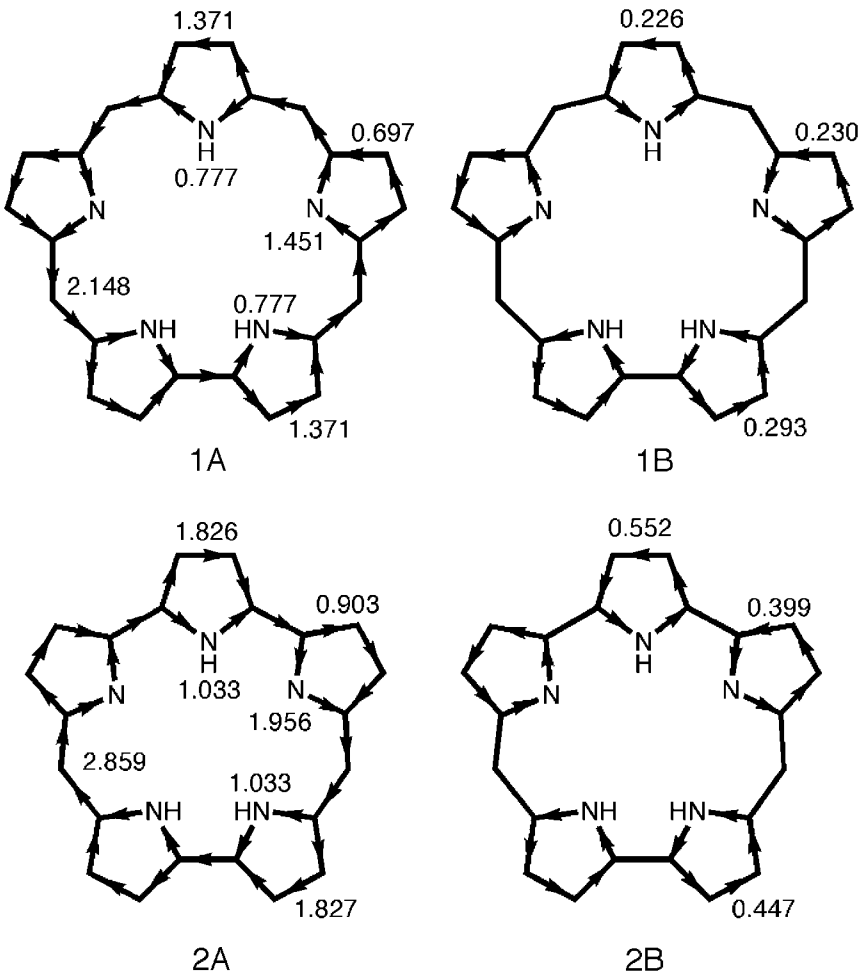

Figure 5. Contributions of macrocyclic (**1A** and **2A**) and five-site (**1B** and **2B**) circuits to the ring currents in **1** and **2**. All current intensities are given in units of the benzene value.

pathways in **1A** and **2A** are identical with the annulene pathways predicted not only by porphyrin chemists[7,11] but also from the BREs. Here, we assume that, to a zeroth-order approximation, all macrocyclic circuits have nearly the same areas. This must be a reasonable assumption for large expanded porphyrins.

Circuit-current magnetic susceptibilities for **1** and **2**, each expressed as a multiple of the benzene value, are also added in Table 2. As circuit-current magnetic susceptibility is proportional to the CRE, weighted with the area of the circuit squared, some large circuits with relatively small CREs may dominate the ring-current magnetic susceptibility. For porphyrins in

general, the most aromatic five-site circuits make the least contribution to ring-current magnetic susceptibility, because they have very small areas.[30] In the case of sapphyrin (**1**), 89% of the MRE arises from five five-site circuits, but these circuits make only a 4% contribution to the ring-current diamagnetic susceptibility. This molecule has ca. 20 times as large a ring-current susceptibility as that for benzene, whereas the TRE is only 2.2 times as large. Ring-current diamagnetic susceptibilities are 20.30 for **1** and −19.59 for **2**, both in units of the benzene value. One should note that the orangarin π-system is paramagnetic with negative ring-current diamagnetic susceptibility, although it is aromatic with a positive TRE. It is obvious that the ring-current magnetic susceptibility or diamagnetic susceptibility exaltation cannot be used as a reliable indicator of global aromaticity for large polycyclic π-systems.

Concluding Remarks

Sapphyrin (**1**) and orangarin (**2**) are moderately aromatic but with small macrocyclic aromaticity and antiaromaticity, respectively. Although macrocyclic aromaticity is energetically negligible, porphyrin chemists have been much interested in its relation to ring-current diamagnetism. We found that the main pathway of π-circulation along the macrocycle is not always the same as that of macrocyclic conjugation. As for **1**, the main macrocyclic conjugation pathway represents the main pathway of macrocyclic π-circulation. However, the main stream of macrocyclic circulation in **2** follows the inner periphery of the π-system, although, according to the annulenoid picture, a main macrocyclic conjugation pathway never passes through amine nitrogens.[21] This problem was solved successfully by excluding local circulation in the pyrrolic rings from the π-current density map. This approach to macrocyclic conjugation must be applicable to many other expanded porphyrins.

This work was supported by a Grant-in-Aid for Scientific Research (No. 16550016) from the Japan Society for the Promotion of Science. Computations were carried out at the Information Processing Center, Shizuoka University, and the Research Center for Computational Science, Okazaki National Research Institutes.

References

1 J. L. Sessler, S. J. Weghorn, *Expanded, Contracted and Isomeric Porphyrins*, Pergamon, New York, **1997**.
2 *The Porphyrin Handbook*, ed. by K. M. Kadish, K. M. Smith, R. Guilard, Academic Press, San Diego, CA, **2000–2003**, Vols. 1–20.
3 J. L. Sessler, D. Seidel, *Angew. Chem., Int. Ed.* **2003**, *42*, 5134.
4 M. J. Broadhurst, R. Grigg, A. W. Johnson, *J. Chem. Soc., Perkin Trans. 1* **1972**, 2111.
5 V. J. Bauer, D. L. J. Clive, D. Dolphin, J. B. Paine, III, F. L. Harris, M. M. King, J. Loder, S.-W. C. Wang, R. B. Woodward, *J. Am. Chem. Soc.* **1983**, *105*, 6429.
6 Z. S. Yoon, S. B. Noh, D.-G. Cho, J. L. Sessler, D. Kim, *Chem. Commun.* **2007**, 2378.
7 J. L. Sessler, S. J. Weghorn, Y. Hiseada, V. Lynch, *Chem.—Eur. J.* **1995**, *1*, 56.
8 E. Vogel, *Pure Appl. Chem.* **1993**, *65*, 143.
9 B. Franck, A. Nonn, *Angew. Chem., Int. Ed. Engl.* **1995**, *34*, 1795.
10 T. D. Lash, *Synlett* **2000**, 279.
11 E. Steiner, P. W. Fowler, *Org. Biomol. Chem.* **2004**, *2*, 34.
12 M. C. Cyrañski, T. M. Krygowski, M. Wisiorowski, N. J. R. van Eikema Hommes, P. v. R. Schleyer, *Angew. Chem., Int. Ed.* **1998**, *37*, 177.
13 J. Jusélius, D. Sundholm, *Phys. Chem. Chem. Phys.* **2000**, *2*, 2145.
14 E. Steiner, P. W. Fowler, *ChemPhysChem* **2002**, *3*, 114.
15 J. Aihara, *J. Am. Chem. Soc.* **1976**, *98*, 2750.
16 I. Gutman, M. Milun, N. Trinajstić, *J. Am. Chem. Soc.* **1977**, *99*, 1692.
17 J. Aihara, *J. Am. Chem. Soc.* **1992**, *114*, 865.
18 J. Aihara, *J. Chem. Soc., Faraday Trans.* **1995**, *91*, 237.
19 J. Aihara, *J. Am. Chem. Soc.* **1995**, *117*, 4130.
20 J. Aihara, *J. Chem. Soc., Perkin Trans. 2* **1996**, 2185.
21 J. Aihara, *J. Phys. Chem. A* **2008**, *112*, 5305.
22 J. Aihara, *J. Am. Chem. Soc.* **1979**, *101*, 5913.
23 J. Aihara, *Pure Appl. Chem.* **1982**, *54*, 1115.
24 J. Aihara, T. Horikawa, *Chem. Phys. Lett.* **1983**, *95*, 561.
25 J. Aihara, *J. Am. Chem. Soc.* **1985**, *107*, 298.
26 J. Aihara, *Bull. Chem. Soc. Jpn.* **2004**, *77*, 651.
27 J. Aihara, *J. Am. Chem. Soc.* **2006**, *128*, 2873.
28 J. Aihara, H. Kanno, T. Ishida, *J. Phys. Chem. A* **2007**, *111*, 8873.
29 J. Aihara, *J. Phys. Chem. A* **2008**, *112*, 4382.
30 J. Aihara, E. Kimura, T. M. Krygowski, *Bull. Chem. Soc. Jpn.* **2008**, *81*, 826.
31 T. Heine, P. v. R. Schleyer, C. Corminboeuf, G. Seifert, R. Reviakine, J. Weber, *J. Phys. Chem. A* **2003**, *107*, 6470.
32 F. London, *J. Phys. Radium* **1937**, *8*, 397.
33 B. Pullman, A. Pullman, *Les Théories Electroniques de la Chimie Organique*, Masson et Cie, Paris, **1952**, Chap. IX.
34 F. A. Van-Catledge, *J. Org. Chem.* **1980**, *45*, 4801.
35 M. J. Frisch, G. W. Trucks, H. B. Schlegel, G. E. Scuseria, M. A. Robb, J. R. Cheeseman, J. A. J. Montgomery, T. Vreven, K. N. Kudin, J. C. Burant, J. M. Millam, S. S. Iyengar, J. Tomasi, V. Barone, B. Mennucci, M. Cossi, G. Scalmani, N. Rega, G. A. Petersson, H. Nakatsuji, M. Hada, M. Ehara, K. Toyota, R. Fukuda, J. Hasegawa, M. Ishida, T. Nakajima, Y. Honda, O. Kitao, H. Nakai, M. Klene, X. Li, J. E. Knox, H. P. Hratchian, J. B. Cross, C. Adamo, J. Jaramillo, R. Gomperts, R. E. Stratmann, O. Yazyev, A. J. Austin, R. Cammi, C. Pomelli, J. W. Ochterski, P. Y. Ayala, K. Morokuma, G. A. Voth, P. Salvador, J. J. Dannenberg, V. G. Zakrzewski, S. Dapprich, A. D. Daniels, M. C. Strain, O. Farkas, D. K. Malick, A. D. Rabuck, K. Raghavachari, J. B. Foresman, J. V. Ortiz, Q. Cui, A. G. Baboul, S. Clifford, J. Cioslowski, B. B. Stefanov, G. Liu, A. Liashenko, P. Piskorz, I. Komaromi, R. L. Martin, D. J. Fox, T. Keith, M. A. Al-Laham, C. Y. Peng, A. Nanayakkara, M. Challacombe, P. M. W. Gill, B. Johnson, W. Chen, M. W. Wong, C. Gonzalez, J. A. Pople, *Gaussian 03, Revision B.02*, Gaussian, Inc., Pittsburgh, PA, **2003**.
36 A. Graovac, I. Gutman, N. Trinajstić, T. Živković, *Theor. Chim. Acta* **1972**, *26*, 67.
37 J. A. Pople, K. G. Untch, *J. Am. Chem. Soc.* **1966**, *88*, 4811.
38 J. A. Pople, *Mol. Phys.* **1958**, *1*, 175.
39 R. McWeeny, *Mol. Phys.* **1958**, *1*, 311.
40 M. Randić, *J. Am. Chem. Soc.* **1977**, *99*, 444.
41 T. Ishida, H. Kanno, J. Aihara, *Pol. J. Chem.* **2007**, *81*, 699.
42 C. A. Coulson, R. B. Mallion, *J. Am. Chem. Soc.* **1976**, *98*,

592.
43 R. B. Mallion, *Pure Appl. Chem.* **1980**, *52*, 1541.
44 J. A. N. F. Gomes, R. B. Mallion, *Chem. Rev.* **2001**, *101*, 1349.
45 E. Steiner, P. W. Fowler, *J. Phys. Chem. A* **2001**, *105*, 9553.
46 E. Steiner, P. W. Fowler, *Chem. Commun.* **2001**, 2220.
47 T. A. Keith, R. F. W. Bader, *Chem. Phys. Lett.* **1993**, *210*, 223.
48 S. Coriani, P. Lazzeretti, M. Malagoli, R. Zanasi, *Theor. Chim. Acta* **1994**, *89*, 181.